ARTICLE

Surface Chemical Modification of Poly(dimethylsiloxane)-Based Biomimetic Materials: Oil-Repellent Surfaces

Nilmoni Ghosh, Arpan Bajoria, and Ashish Anant Vaidya*

Unilever Research India, 64 Main Road, Whitefield, Bangalore, India

ABSTRACT The oil-repellent performance of a poly(dimethylsiloxane)-based biomimetic replica (PDMS-replica) was tuned by modifying its surface chemical composition. PDMS-replica possessing a complementary combination of hierarchical roughness and mixed $-CF_3$ and $-SiCH_3$ terminal functionality was prepared in the presence of a surface-modifying agent, using nanocasting based on soft lithography. PDMS-replica showed superhydrophobicity and enhanced oil repellency, $\theta_{oil} \sim 86°$. PDMS-replica was further modified with silica nanoparticles followed by chemical vapor deposition of (heptadecafluoro-1,1,2,2-tetrahydrodecyl)trichlorosilane. The $-CF_3$ terminal, silica-modified PDMS-replica (i.e., PDMS-replica$^{silica/CF_3}$) showed both superhydrophobic and high oil-repellent properties (advancing $\theta_{oil} \sim 120°$). During the process of each chemical transformation, the surface pattern present on PDMS-replica was preserved and monitored using scanning electron microscopy. Surface chemical compositions of PDMS-replica and PDMS-replica$^{silica/CF_3}$ were determined using X-ray photoelectron spectroscopy. Understanding the extent of adhesion on a biomimetic replica possessing different surface chemical compositions and roughness would provide fundamental information for various applications.

KEYWORDS: oil repellency • superoleophobic • artificial leaf • surface modification • biomimetic • nanocasting • soft lithography

BACKGROUND

Superhydrophobic materials are emerging in many industrial and biological applications, such as self-cleaning/antistick (1−4) and antifouling (5−7) coatings. Most of these materials (8−10) were fabricated by mimicking micrometer- and nanometer-sized hierarchical asperities present on a self-cleaning leaf surface (11, 12). Nanocasting based on soft lithography (13, 14) was used to fabricate superhydrophobic biomimetic materials, using a natural leaf template (15). In this process, a reactive poly(dimethylsiloxane) (PDMS) blend was applied on a leaf template, followed by curing it into the solid film. During the process of solidification, the complement of the leaf's surface pattern was transferred on the solid negative replica. Similarly, a negative replica was used as the template to develop a superhydrophobic positive PDMS-replica. Previously reported replicas (3−5, 16−24) did not exhibit oil-repellent properties. Also, the extent of oil repellency on such replicas possessing a complementary combination of hierarchical surface roughness and chemical constitution has not been studied so far.

Fundamentally (25−29), oil repellency attributes to the close-packed $-CF_3$ terminal functionality having a surface energy (γ_s) of ~10 mJ/m^2. Most of the oil with a surface tension (γ_{oil}) of 36 mJ/m^2 would exhibit a maximum contact angle (θ_{oil}) of 87° on a flat solid surface if the dispersion component of the solid surface energy (γ_s) is expressed by the equation (30−32) $\gamma_s = \gamma_{oil}(1 + \cos\theta_{oil})^2/4$. Furthermore, oil repellency can be achieved only through a complementary combination of the $-CF_3$ terminal functionality and hierarchical surface roughness (33−40). McKinley and Cohen fabricated superoleophobic surfaces through a unique combination of the $-CF_3$ terminal functionality and "reentrant texture" (i.e., nanoscale concave structural topography) (41, 42). These surfaces were prepared by electrospinning of a polymer blend of fluoro polyhedral oligomeric silsesquioxane and poly(methyl methacrylate) into a nonwoven bristle like a microhoodoo structure etched on the silicon metal. Gao et al. (43) developed oil-repellent surfaces by fabricating a hierarchical porous structure, followed by depositing tridecafluoro-1,1,2,2-tetrahydrooctyltrichlorosilane (n-$C_6F_{13}CH_2CH_2SiCl_3$) on a silicon film. A similar concept was used to achieve oil repellency on cotton (44−47), cellulose (48, 49), and wool (50) through in situ deposition of fluorinated silica particles.

The limited oil repellency of PDMS-replica (15) was presumably be due to the $-SiCH_3$ terminal functionality (51, 52), which attributed to a surface energy of 22 mJ/m^2. Our objective was to develop oil-repellent PDMS-replica via a surface chemical modification approach. Our approach was to replace the surface terminal $-SiCH_3$ of PDMS-replica with $-CF_3$ groups by preserving its original hierarchical micrometer- and nanometer-sized surface pattern. Conventionally, chemical modification of a flat PDMS film was achieved via plasma oxidation followed by the formation of self-assembled monolayers (SAMs) (53−57). However, plasma oxidation has shown evidence of surface topographical alteration or damage on flat PDMS films (58). It is therefore practically challenging to modify PDMS-replica in

* To whom correspondence should be addressed. E-mail: ashish.vaidya@unilever.com. Tel: +91-080-39830994.
Received for review July 15, 2009 and accepted October 5, 2009

DOI: 10.1021/am9004732
© 2009 American Chemical Society

Published on Web 10/28/2009

a similar manner because plasma could damage its delicate surface asperities. Indeed, our data showed that prolonged wet oxidation caused damage to the micrometer- and nanometer-sized hierarchical asperities present on PDMS-replica (as described in the Results and Discussion).

In this paper, we demonstrate the preparation of oil-repellent PDMS-replica possessing a $-CF_3$ terminal functionality and a hierarchical surface pattern. PDMS-replica was first prepared in the presence of a surface-modifying fluorocarbon agent, using nanocasting based on soft lithography. During the casting process, the fluorocarbon was expected to segregate and embed in the surface composition of PDMS-replica. Surface-modified PDMS-replica possessing a complementary combination of hierarchical roughness and mixed $-CF_3$ and -$SiCH_3$ terminal functionality showed oil repellency ($\theta_{oil} \sim 86°$). This oil-repellent performance of PDMS-replica was further enhanced by fully replacing $-SiCH_3$ terminal groups with $-CF_3$. PDMS-replica was further modified with silica nanoparticles, followed by chemical vapor deposition of (heptadecafluoro-1,1,2,2-tetrahydrodecyl)trichlorosilane. The $-CF_3$ terminal, silica-modified PDMS-replica (i.e., PDMS-replica$^{silica/CF_3}$) showed both superhydrophobic and high oil-repellent properties (advancing $\theta_{oil} \sim 120°$). During the process of each chemical transformation, the micrometer- and nanometer-sized surface pattern present on PDMS-replica was preserved and monitored using scanning electron microscopy (SEM). The surface chemical compositions of PDMS-replica and PDMS-replica$^{silica/CF_3}$ were determined using X-ray photoelectron spectroscopy (XPS).

EXPERIMENTAL SECTION

Materials. (Heptadecafluoro-1,1,2,2-tetrahydrodecyl)trichlorosilane [99%, having molecular formula $Cl_3Si(CH_2)_2(CF_2)_7CF_3$] was purchased from Gelest and used as the freshly prepared 0.1% active solution in dry paraffin oil (Aldrich). Sylgard-184 was purchased from Dow Corning. Tetraethyl orthosilicate (98%), hydrogen peroxide (30%), and an ammonia solution (30%) were purchased from Sigma-Aldrich.

Preparation of PDMS-Replica Using Colocasia Leaf. Fresh colocasia leaf (facing the bottom part upward) was placed in a polystyrene Petri dish (100 × 15 mm). The reactive PDMS blend was prepared by mixing a silicone elastomer base and a curing agent (Sylgard-184) in a weight ratio of 10:1 (59). The viscous blend was poured onto a leaf placed in a Petri dish. The trapped air bubbles were removed by applying a gentle vacuum (100 mm) for 15−20 min. When the blend was completely free of air bubbles, it was cured at 25 °C in a dust-free chamber for approximately 24 h. The solid negative replica of the leaf (negative PDMS-replica; area ∼6−8 cm^2, thickness ∼2−5 mm) was kept in the oven at 60 °C for 1 h. It was peeled carefully from the leaf, washed gently with distilled water, and purged with nitrogen. The negative PDMS-replica was transferred into a chamber, where it was exposed to the vapors of (heptadecafluoro-1,1,2,2-tetrahydrodecyl)trichlorosilane for 1 h, under reduced pressure (∼1 mmHg). The fluorocarbon-coated negative PDMS-replica (facing the negatively patterned surface upward) was placed in a polystyrene Petri dish (100 × 15 mm). The reactive PDMS blend was again poured on the fluorocarbon-coated negative PDMS-replica. The blend was cured and peeled from it to obtain PDMS-replica.

Preparation of $-CF_3$ Terminal, Silica-Modified PDMS-Replica (PDMS-Replica$^{silica/CF_3}$). PDMS-replica (area ∼4 cm^2 and thickness ∼5 mm) was treated with a mixture of hydrogen peroxide (30%, 1 part), hydrochloric acid (36%, 1 part), and water (2 parts) for 10 min. The oxidized PDMS-replica (i.e., PDMS-replica^{OH}) was washed with distilled water and purged with nitrogen gas. The dry PDMS-replica^{OH} was immediately treated with a sol−gel mixture of tetraethyl orthosilicate (1 part), ammonia (1 part), and ethanol (15 parts). The mixture was left undisturbed for 2 h. The silica-modified positive replica (PDMS-replica^{silica}) was washed with ethanol and purged with nitrogen gas. The dry PDMS-replica^{silica} was immediately transferred into a chamber, where it was exposed to the vapors of (heptadecafluoro-1,1,2,2-tetrahydrodecyl)trichlorosilane for 1 h, under reduced pressure (∼1 mmHg). After curing at 60 °C for about 1 h, the adsorbed chlorosilane was assumed to react with the silanol groups present on PDMS-replica^{silica} to yield $-CF_3$ terminal, silica-modified positive replica (PDMS-replica$^{silica/CF_3}$). Both CF_3 terminal, flat PDMS (PDMS^{CF3}) and silica-modified PDMS (PDMS$^{silica/CF_3}$) films were prepared using a similar procedure.

SEM of PDMS-Replicas. Topographical changes on surface-modified PDMS-replica were evaluated with a Hitachi S-47 field-emission scanning electron microscope using an acceleration potential of 10 kV. Before imaging, the replicas were sputter-coated with a gold layer of thickness 50 nm using a Hitachi capital ε-1010 ion sputter coater (operation parameters: working pressure 0.05 mbar, distance 50 mm, current 30 mA, and time 120 s).

Wettability Method. Contact angles were measured at room temperature with a Kruss (GmbH Germany) G 10 goniometer. The advancing and receding contact-angle measurements of water on replica surfaces were carried out using a sessile-drop technique (60). The contact angles with the replica film surface were measured using a telescope fitted with a video camera. The advancing and receding contact angles were recorded by continuously supplying and withdrawing water through the needle, respectively. The aqueous stain solutions were prepared by dissolving 0.001% methylene blue in water. The static contact-angle measurement of oil (glyceryl trioleate) on the replica surfaces was carried out using a sessile-drop technique.

XPS. The surface chemical compositions of PDMS-replica and PDMS-replica$^{silica/CF_3}$ were determined using XPS with a ESCA-3000 instrument (VG Scientific, U.K.). X-rays were generated using a water-cooled high-intensity rotating Al Kα source, at a power of 150 W. The thin films of replica (area 1 cm^2 and thickness 5 mm) were used for XPS analysis. The pass energy of 50 eV was used for survey spectra. For the high-resolution spectra, Si 2p (102 eV), Si 2s (152 eV), C 1s (284 eV), O 1s (532 eV), and F 1s (688 eV) regions were acquired with a pass energy of 50 eV at a 90° takeoff angle. Spectra were interpreted by referring to the Scienta ESCA300 database (61, 62). The Gaussian peak deconvolution analysis was performed using Peak fit v4.11 software (SPSS Inc.).

RESULTS AND DISCUSSION

Superhydrophobic and Oil-Repellent PDMS-Replica. The superhydrophobic property of self-cleaning plants is well-known because of the hierarchical micrometer- and nanometer-sized pattern present on their leaf surface. A typical SEM of the bottom side of the dry natural colocasia leaf observed under low vacuum revealed the presence of a periodic array of flower-shaped protuberance, as shown in Figure 1A. The magnified SEM image in Figure 1B indicates that each protuberance has an average diameter of 12 μm with a special distance of ∼20 μm between them. A further magnified SEM image in Figure 1C shows that the individual flower-shaped protuberances possessed a fiberlike mesh structure, with an average fiber width of less than a micrometer. The optical picture of a water drop (containing

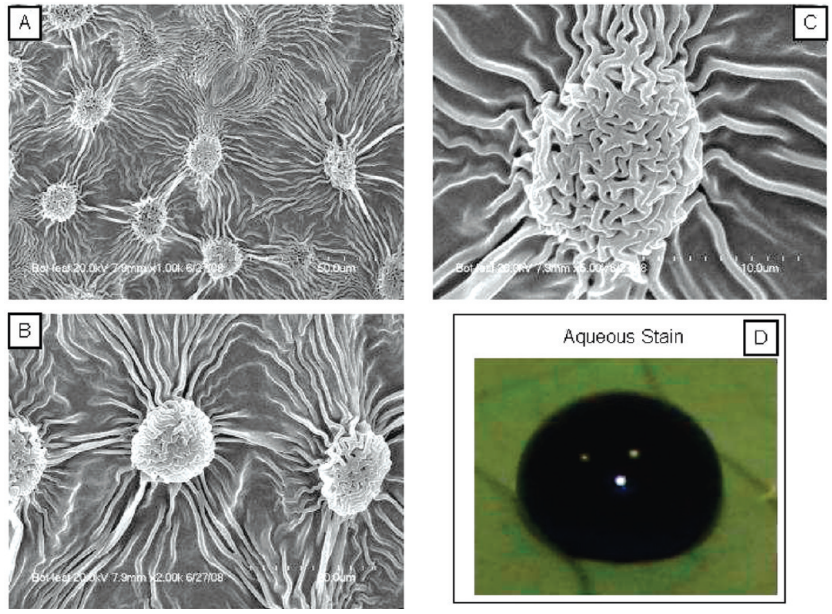

FIGURE 1. SEM images of the bottom side of a dry colocasia leaf showing (A) an array of flower-shaped protuberances (scale bar 50 μm), (B) a pair of protuberances (scale bar 20 μm), (C) a fiberlike mesh structure present on each protuberance (scale bar 10 μm), and (D) an optical picture of a water drop (containing 0.001% methylene blue) on the bottom side of the colocasia leaf surface.

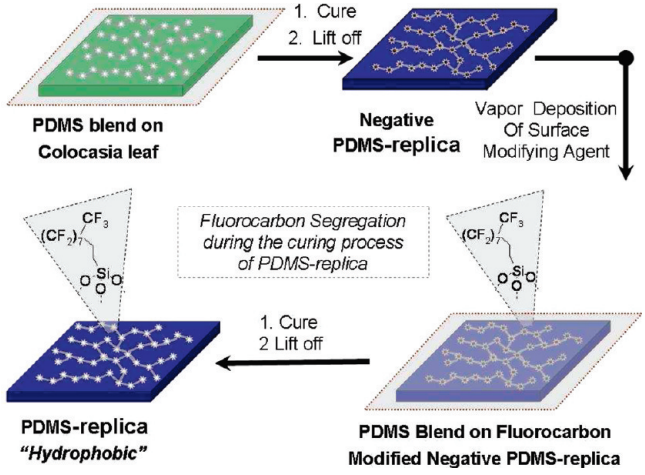

FIGURE 2. Preparation of a positive replica of a colocasia leaf (PDMS-replica).

0.001 % methylene blue) on the bottom side of the colocasia leaf surface is shown in Figure 1D.

Hang et al. (15) described the fabrication of PDMS-replica using nanocasting based on soft lithography. As described in Figure 2, we applied a reactive PDMS blend on the bottom side of a fresh colocasia leaf. During the process of solidification, it was assumed that the complement of the original leaf's surface pattern would transfer onto the solid negative replica.

A typical SEM (Figure 3A) of negative PDMS-replica observed at low vacuum showed a hierarchical array of pits originating from the flower-shaped protuberance present on the leaf surface, as shown in Figure 1A,B. The diameter of each pit was about 10 μm with a special distance of about 25 μm between them. The magnified SEM image in Figure 3B revealed that the pit wall and its vicinity area were patterned with an array of channels originating from the fiberlike mesh structure present on each protuberance of leaf (Figure 1C). The channel width was found to be less than a micrometer.

Next, we deposited a monolayer of the (heptadecafluoro-1,1,2,2-tetrahydrodecyl)trichlorosilane release agent on the negative PDMS-replica surface. The reactive PDMS blend was applied on a fluorocarbon-modified negative PDMS-replica. During the process of solidification, it was assumed that the complement of a negative PDMS-replica surface pattern would transfer on the solid positive replica. Also, the fluorocarbon release agent present on negative PDMS-replica was expected to segregate and embed in the surface composition of PDMS-replica. Hence, the PDMS-replica surface was found to be modified with fluorocarbon, which showed enhanced oil repellency.

The surface topography of PDMS-replica (Figure 3C,D) was similar to that of a natural colocasia leaf (Figure 1C). A typical SEM (Figure 3C) of the positive replica (PDMS-replica) observed at low vacuum showed a hierarchical array of flower-shaped protuberances originating from the pits present on negative PDMS-replica, as shown in Figure 3A. It also indicates that each protuberance has an average diameter of 12 μm with a special distance of ~20 μm between them. The magnified SEM image in Figure 3D revealed that the individual flower-shaped protuberances possessed a fiberlike mesh structure originating from the channels present on the pit wall, as shown in Figure 3B. The fiber width was found to be less than a micrometer.

Surface Chemical Composition and Wettability of PDMS-Replica. Both a natural colocasia leaf as well as an artificial leaf (PDMS-replica) offered advancing and receding contact angles (θ_{water}) of ~150° and 140°, respectively, with water. We observed low contact angles of oil on both flat PDMS and negative PDMS-replica ($\theta_{oil} \sim 45°$) presumably because of the presence of $-SiCH_3$ terminal groups. Our previous XPS studies (52) indicated that the

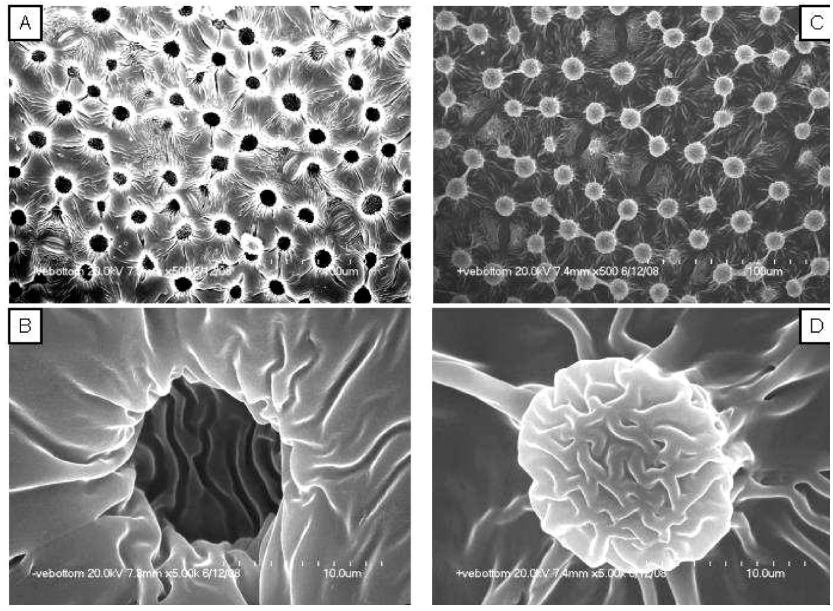

FIGURE 3. SEM images of (A) an array of pits present on negative PDMS-replica (scale bar 100 μm), (B) a channellike structure present on the pit wall and its vicinity (scale bar 10 μm), (C) an array of flower-shaped protuberances present on PDMS-replica (scale bar 100 μm), and (D) a fiberlike mesh structure present on each protuberance and its vicinity (scale bar 10 μm).

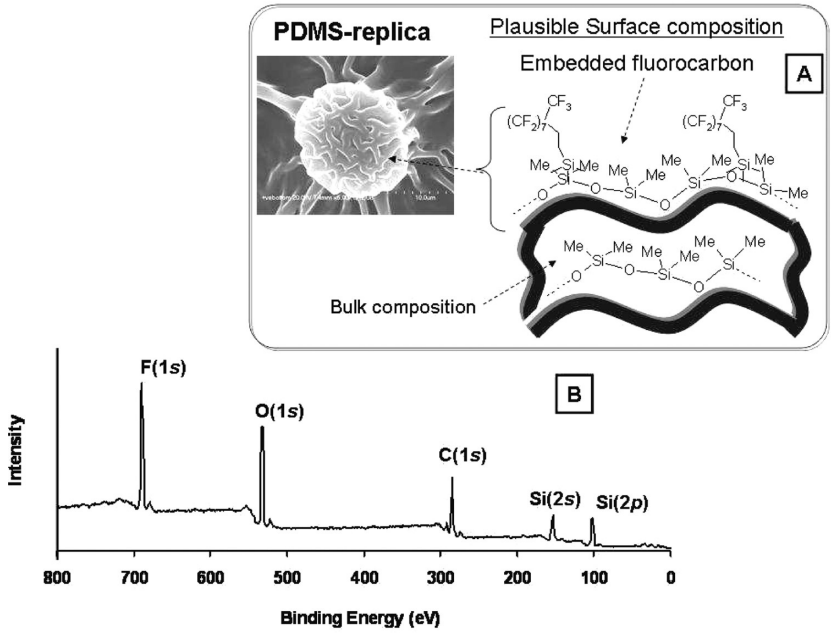

FIGURE 4. (A) Plausible surface and bulk chemical composition of PDMS-replica. (B) XPS survey spectrum at a 90° takeoff angle from PDMS-replica.

PDMS films possess $-SiCH_3$ terminal groups, which attribute to a surface energy of ~22 mJ/m^2. Interestingly, relatively higher contact of oil was observed on PDMS-replica ($\theta_{oil} \sim$ 86°) than on flat PDMS and negative PDMS-replica. This was observed to be due to the presence of embedded fluorocarbon in the surface composition of PDMS-replica. A plausible surface and bulk chemical composition of modified PDMS-replica is shown in Figure 4A. The surface chemical composition of PDMS-replica was determined using XPS. In Figure 4B, XPS survey spectrum of PDMS-replica shows peaks at 688, 532, 284, 152, and 102 eV due to F 1s, O 1s, C 1s, Si 2s, and Si 2p, respectively.

High-resolution spectra of Si 2p (102 eV), C 1s (284 eV), O 1s (532 eV), and F 1s (688 eV) regions are shown in Figure 5. The peak corresponding to a C atom bound to a H atom, specifically the signals due to the *C*—H groups present in the PDMS segments, appeared at 284.15 eV. In addition, relatively low intensity peaks corresponding to a C atom bonded to a F atom, specifically $-SiCH_2CH_2(CF_2)_7CF_3$ and $-SiCH_2CH_2$-$(CF_2)_7CF_3$, appeared at 291.26 and 292.4 eV, respectively. The peaks corresponding to Si and O atoms, specifically signals due to *Si*—*O* groups present in the PDMS segments, appeared at 101.8 (Si 2p) and 532.09 (O 1s) eV, respectively. A relatively low intensity peaks corresponding to *Si*—*O*

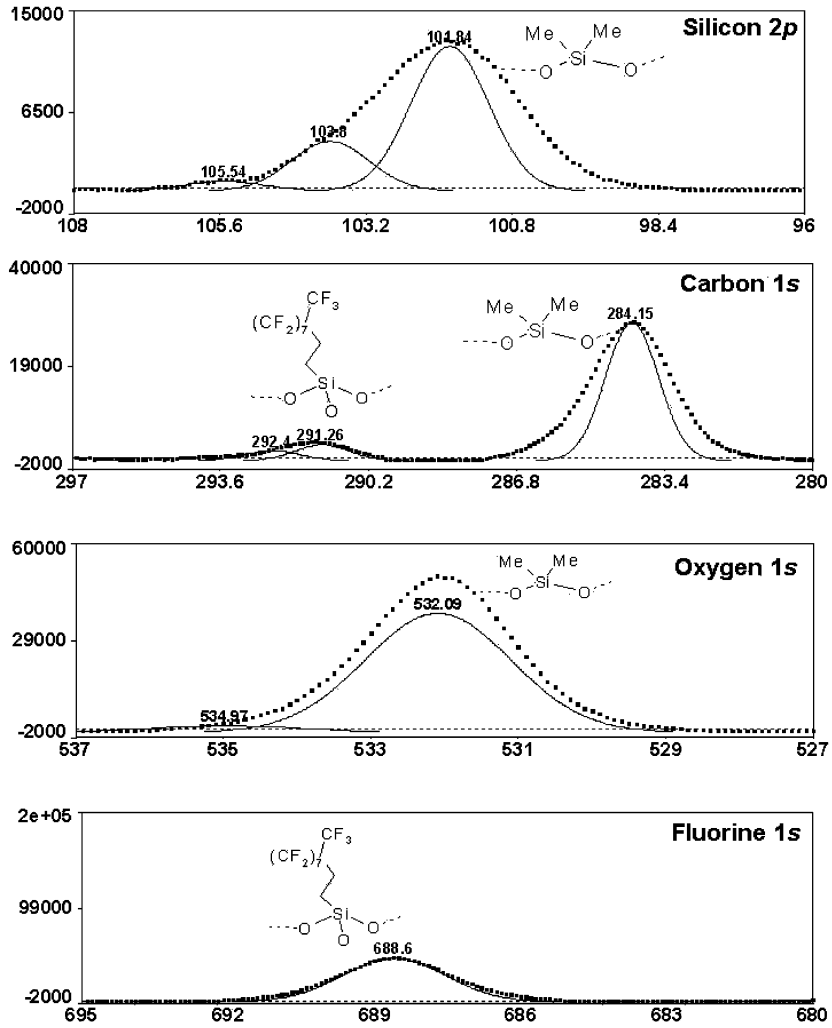

FIGURE 5. XPS spectra of the Si 2p, C 1s, O 1s, and F 1s regions at 90° takeoff angle from PDMS-replica: (- - -) data; (—) Gaussian sum.

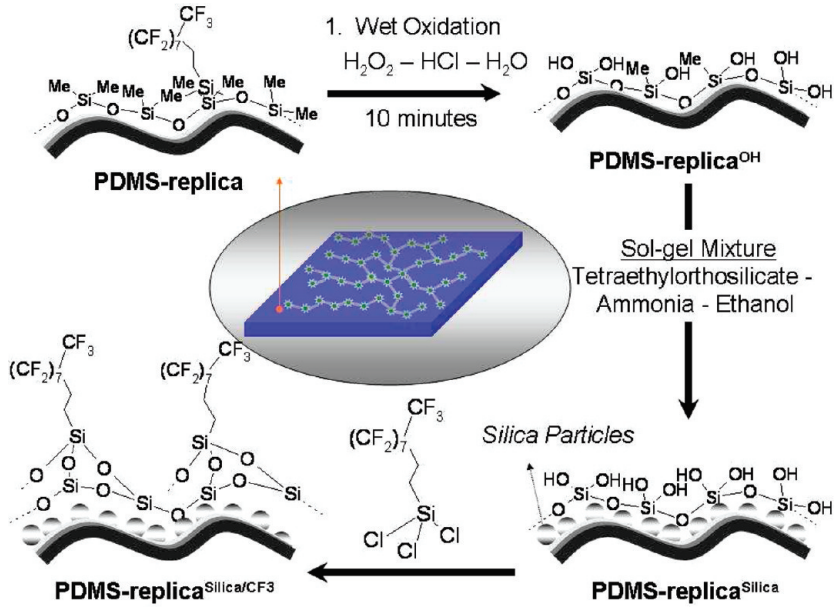

FIGURE 6. Surface chemical modification of PDMS-replica to PDMS-replica$^{silica/CF_3}$.

groups, specifically the $-(O)_3SiCH_2(CF_2)_7CF_3$ network, appeared at 103.8 eV. Also, a peak corresponding to a F atom, specifically $-(CH_2)(CF_2)_7CF_3$, appeared at 688.6 eV. Interestingly, XPS data obtained from PDMS-replica revealed the presence of both $-CF_3$ and $-SiCH_3$ terminal functional groups on its surface. Hence, PDMS-replica offered en-

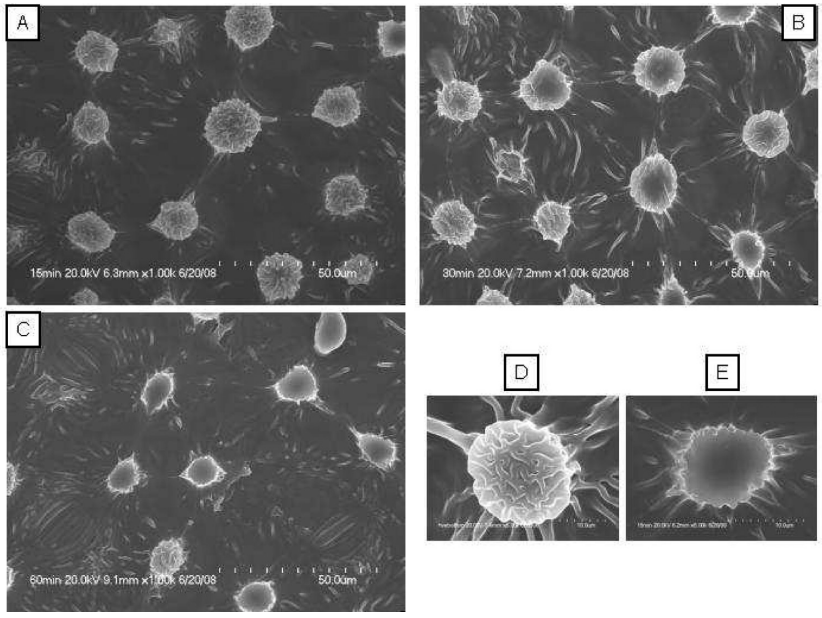

FIGURE 7. SEM images of surface patterns present on PDMS-replica after treatment with an oxidizing solution for (A) 15, (B) 30, and (C) 60 min. Magnified SEM images of surface patterns present on PDMS-replica (D) before and (E) after treatment with an oxidizing solution for 60 min.

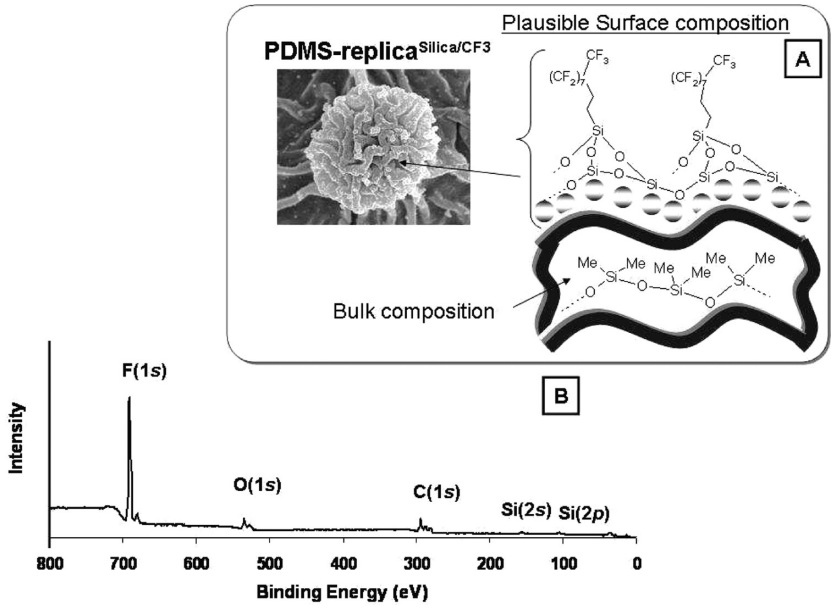

FIGURE 8. (A) Plausible surface and bulk chemical composition of PDMS-replica$^{silica/CF_3}$. (B) XPS survey spectrum at a 90° takeoff angle from PDMS-replica$^{silica/CF_3}$.

hanced oil repellency, although it did not meet our expectation of superoleophobicity. Therefore, further high oil repellency on PDMS-replica can be achieved only if $-SiCH_3$ terminal groups are fully replaced with $-CF_3$ by preserving its original hierarchical micrometer- and nanometer-sized surface pattern.

Oil-Repellent PDMS-Replica$^{silica/CF_3}$ via Chemical Functionalization of PDMS-Replica. Surface chemical modification of a flat PDMS film was achieved by forming a SAM of organosilanes on its plasma-oxidized surface (53−57). Plasma surface modification provides an interfacial chemical structure like silica on PDMS that is suitable for chemical functionalization (63). We had initially planned surface modification of PDMS-replica through plasma oxidation. However, it is known that plasma oxidation alters the surface topography of flat PDMS films (58). We therefore did not rule out the possibility that plasma oxidation could damage or alter the hierarchical micrometer- and nanometer-sized pattern already present on the PDMS-replica surface.

Chemical functionalization of PDMS-replica was therefore performed via a mild wet oxidation treatment (64). As indicated in Figure 6, PDMS-replica was treated with an oxidizing solution for different times. Undesirable topographical surface changes occurring on PDMS-replica because of the wet oxidation treatment were monitored using SEM.

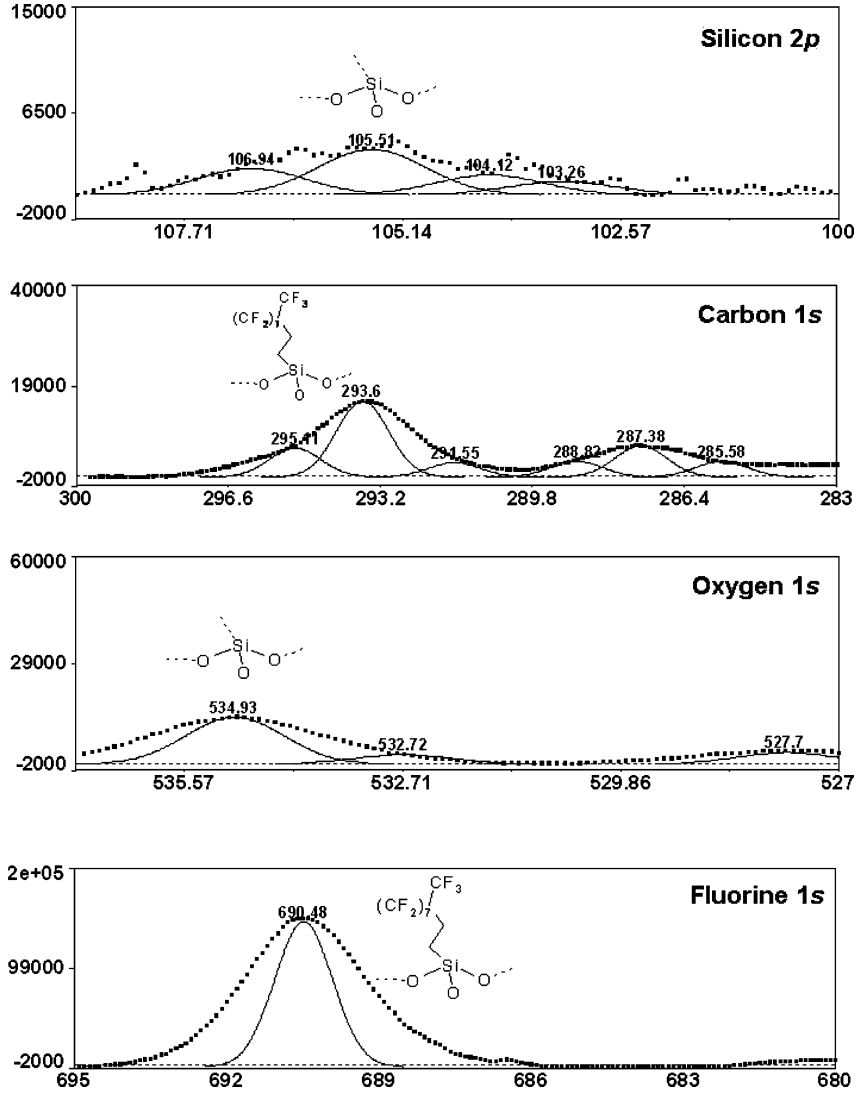

FIGURE 9. XPS spectra of Si 2p, C 1s, O 1s, and F 1s regions at a 90° takeoff angle from PDMS-replica$^{silica/CF_3}$: (- - -) data; (—) Gaussian sum.

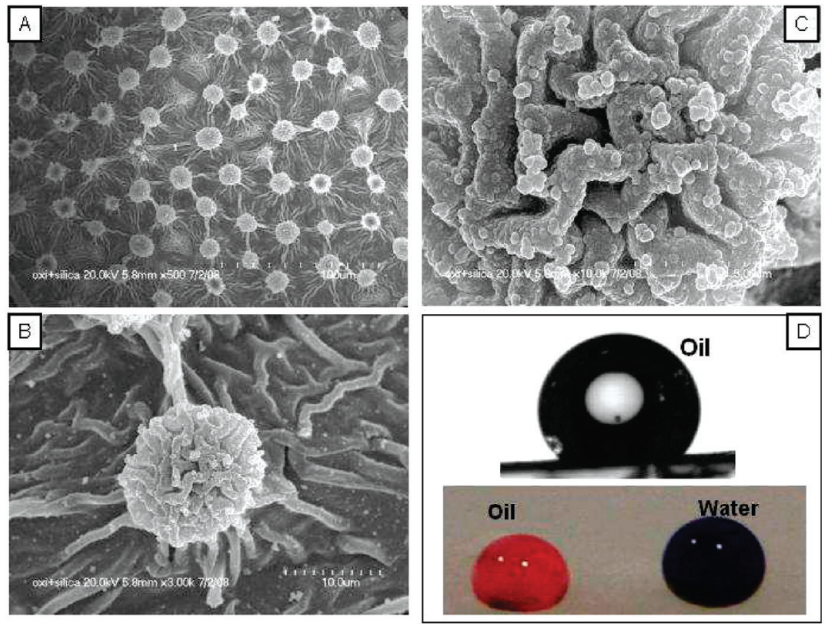

FIGURE 10. SEM images of PDMS-replica$^{silica/CF_3}$ showing (A) an array of flower-shaped protuberances (scale bar 100 μm), (B) silica-modified protuberances (scale bar 10 μm), (C) a silica-modified fiberlike mesh structure present on each protuberance (scale bar 5 μm), and (D) a goniometer telescope−video image of oil and optical images of oil and water drops on the PDMS-replica$^{silica/CF_3}$ surface.

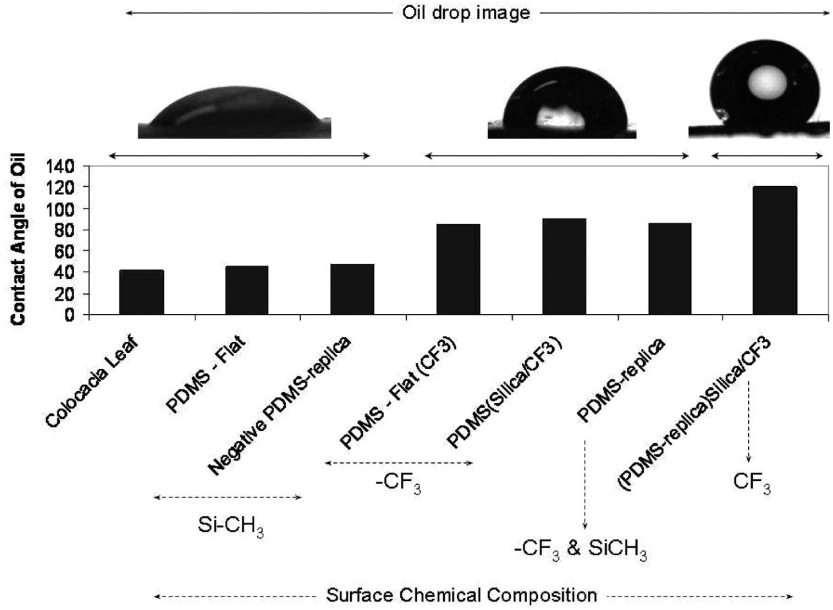

FIGURE 11. Contact angles and goniometer telescope–video images of oil on various patterned and nonpatterned surfaces.

Different surface morphologies of PDMS-replica obtained after treatment with an oxidizing solution for 15, 30, and 60 min are shown in Figure 7A–C. We observed that prolonged treatment of PDMS-replica with an oxidizing solution partly, or in some cases fully, damaged the nanometer-sized fiberlike mesh structure. Figure 7E reveals a magnified image of a completely damaged fiberlike mesh structure present on the protuberance after 60 min of treatment with an oxidizing solution. Optimized oxidation treatment for only 10 min turned PDMS-replica hydrophilic, showing an advancing contact angle of water ($\theta_{water} \sim 35°$). The surface hydrophilicity reflected the formation of silanol (Si–OH) groups on the oxidized PDMS-replica surface. As shown in Figure 6, oxidized PDMS-replica (PDMS-replica^{OH}) was treated with a sol–gel mixture (65, 66) of ethanol, tetraethyl orthosilicate, ammonia, and ethanol with a volume ratio of 1:1:15, respectively, for 2 h. This treatment triggered the formation of nanosilica particles on the PDMS-replica^{OH} surface. The silanol-terminated, silica-modified PDMS-replica (PDMS-replica^{silica}) was immediately treated with (heptadecafluoro-1,1,2,2-tetrahydrodecyl)trichlorosilane under vacuum. The adsorbed chlorosilane was intended to react with the silanol groups present on PDMS-replica^{silica} to yield PDMS-replica$^{silica/CF_3}$.

Surface Chemical Composition and Wettability of Oil-Repellent PDMS-Replica$^{silica/CF_3}$. Surface compositions of PDMS-replica$^{silica/CF_3}$ were determined using XPS. The plausible surface and bulk chemical composition of PDMS-replica$^{silica/CF_3}$ is shown in Figure 8A. The presence of a $-CF_3$ terminal functionality on the PDMS-replica$^{Silica/CF3}$ surface was confirmed by XPS. In Figure 8B, the XPS survey spectrum of PDMS-replica$^{silica/CF_3}$ shows an intense peak at 690 eV due to F 1s along with relatively low intensity peaks at 535, 290, 157, and 105 eV due to O 1s, C 1s, Si 2s, and Si 2p, respectively. The F 1s peak was observed because of the presence of fluorocarbon SAMs on PDMS-replica$^{silica/CF_3}$.

High-resolution spectra of Si 2p (105 eV), C 1s (290 eV), O 1s (535 eV), and F 1s (690 eV) regions are indicated in Figure 9. The intensities of the strong peaks at 101.8 (Si 2p), 284.14 (C 1s), and 532.09 (O 1s) eV corresponding to the terminal $-Si(CH_3)_2O-$ groups from PDMS-replica decreased dramatically because of deposition of the CF_3 terminal silica network on its surface.

The additional peak corresponding to a C atom bonded to a F atom, specifically $-SiCH_2CH_2CF_2(\mathit{C}F_2)_6CF_3$, appeared at 293.6 eV. The relatively low intensity peaks due to $-SiCH_2CH_2CF_2(CF_2)_6\mathit{C}F_3$, $-SiCH_2CH_2\mathit{C}F_2(CF_2)_6CF_3$, $-SiCH_2\text{-}\mathit{C}H_2CF_2(CF_2)_6CF_3$, and $-Si\mathit{C}H_2CH_2CF_2(CF_2)_6CF_3$ appeared at 295.1, 291.5, 288.8 and 287.3 eV, respectively. The peaks corresponding to Si and O atoms, specifically signals due to *Si–O* groups in the silica network, appeared at 105.5 (Si 2p) and 534.92 (O 1s) eV, respectively. Also, a peak corresponding to a F atom, specifically $-CH_2(CF_2)_7CF_3$, appeared at 690 eV. SEM analysis of PDMS-replica$^{silica/CF_3}$ showed an intact hierarchical array of flower-shaped protuberances (Figure 10A). The magnified SEM image in Figure 10B revealed that the individual flower-shaped protuberances possessed a silica-coated fiberlike mesh structure. The further magnified SEM image in Figure 10C showed that each fiber was coated with silica having an average particle size of less than 400 nm. PDMS-replica$^{silica/CF_3}$ showed both superhydrophobic (advancing $\theta_{water} \sim 155°$ and receding $\theta_{water} \sim 142°$) and high oil-repellent properties (advancing $\theta_{oil} \sim 120°$ and receding $\theta_{oil} \sim 102°$) in Figure 10D.

A theoretical correlation of the surface roughness, chemical composition, and oil repellency is not yet understood. We presume that this system fits in a mixture of Wenzel (67) (penetration) and Cassie–Baxter (suspension) (68) states. A summary of the goniometer telescope–video images of oil on various types of oil surfaces is shown in Figure 11.

SUMMARY

The oil-repellent performance of biomimetic PDMS-replica was tuned by modifying its surface chemical composition. The reactive nanosilica particles were generated on a mild oxidized PDMS-replica surface, followed by deposition of (heptadecafluoro-1,1,2,2-tetrahydrodecyl)trichlorosilane. The $-CF_3$ terminal, silica-modified PDMS-replica showed both superhydrophobic ($\theta_{water} \sim 155°$) and high oil-repellent properties (advancing $\theta_{oil} \sim 120°$). Polymeric materials possessing a desired surface energy and biomimetic roughness were prepared using a simple and cost-effective approach. This type of performance could be useful in various surface applications including nonstick coatings, fouling-resistant coatings, paints, and adhesives.

Acknowledgment. Arpan Bajoria thankfully acknowledges Unilever Research India for the summer project funding. We are thankful to Praveenkumar Nyalam and Dr. Venkat Shankar (Measurement Science, Bangalore) for SEM imaging and XPS facility. We are also grateful to Chemistry (Science) group for the valuable discussions.

REFERENCES AND NOTES

(1) Mitchinson, A. *Nature* **2007**, *445* (7126), 373.
(2) Feng, X. J.; Jiang, L. *Adv. Mater.* **2006**, *18*, 3063.
(3) Nosonovsky, M. *Langmuir* **2007**, *23* (6), 3157.
(4) Qu, M. N.; Zhao, G. Y.; Cao, X. P.; Zhang, J. Y. *Langmuir* **2008**, *24* (8), 4185.
(5) Genzer, J.; Efimenko, K. *Biofouling* **2006**, *22* (5), 339.
(6) Silverman, H. G.; Roberto, F. F. *Mar. Biotechnol.* **2007**, *9* (6), 661.
(7) Waite, J. H.; Andersen, N. H.; Jewhurst, S.; Sun, C. J. *J. Adhes.* **2005**, *81* (3−4), 297.
(8) Furstner, R.; Barthlott, W.; Neinhuis, C.; Walzel, P. *Langmuir* **2005**, *21* (3), 956.
(9) Singh, R. A.; Yoon, E. S. *J. Korean Phys. Soc.* **2008**, *52* (3), 656.
(10) Singh, R. A.; Yoon, E. S.; Kim, H. J.; Kim, J.; Jeong, H. E.; Suh, K. Y. *Mater. Sci. Eng., C* **2007**, *27* (4), 875.
(11) Barthlott, W.; Neinhuis, C. *Planta* **1997**, *202*, 1.
(12) Blossey, R. *Nat. Mater.* **2003**, *2*, 301.
(13) Whitesides, G. M.; Ostuni, E.; Takayama, S.; Jiang, X. Y.; Ingber, D. E. *Annu. Rev. Biomed. Eng.* **2001**, *3*, 335.
(14) Xia, Y. N.; Whitesides, G. M. *Annu. Rev. Mater. Sci.* **1998**, *28*, 153.
(15) Sun, M.; Luo, C.; Xu, L.; Ji, H.; Ouyang, Q.; Yu, D.; Chen, Y. *Langmuir* **2005**, *21* (19), 8978.
(16) Li, X.-M.; Reinhoudt, D.; Crego-Calama, M. *Chem. Soc. Rev.* **2007**, *36*, 1350.
(17) Koch, K.; Schulte, A. J.; Fischer, A.; Gorb, S. N.; Barthlott, W. *Bioinspiration Biomimetics* **2008**, *3*, 1.
(18) Schulte, A. J.; Koch, K.; Spaeth, M.; Barthlott, W. *Acta Biomater.* **2009**, *5* (6), 1848.
(19) Koch, K.; Bhushan, B.; Jung, Y. C.; Barthlott, W. *Soft Matter* **2009**, *5*, 1386.
(20) Roach, P.; Shirtcliffe, N. J.; Newton, M. I. *Soft Matter* **2008**, *4* (2), 224.
(21) Erbil, H. Y.; Demirel, A. L.; Avci, Y.; Mert, O. *Science* **2003**, *299* (5611), 1377.
(22) Yuan, Z. Q.; Chen, H.; Tang, J. X.; Gong, H. F.; Liu, Y. J.; Wang, Z. X.; Shi, P.; Zhang, J. D.; Chen, X. *J. Phys. D: Appl. Phys.* **2007**, *40*, 3485.
(23) Jiang, L.; Zhao, Y.; Zhai, J. *Angew. Chem., Int. Ed.* **2004**, *43* (33), 4338.
(24) Miyauchi, Y.; Ding, B.; Shiratori, S. *Nanotechnology* **2006**, *17* (20), 5151.
(25) Thanawala, S. K.; Chaudhury, M. K. *Langmuir* **2000**, *16* (3), 1256.
(26) Sawada, H.; Ikematsu, Y.; Kawase, T.; Hayakawa, Y. *Langmuir* **1996**, *12* (15), 3529.
(27) Schmidt, D. L.; Coburn, C. E.; Dekoven, B. M.; Potter, G. E.; Meyers, G. F.; Fischer, D. A. *Nature* **1994**, *368*, 39.
(28) Schmidt, D. L.; Coburn, C. E.; Dekoven, B. M.; Potter, G. E.; Meyers, G. F.; Fischer, D. A. *Langmuir* **1996**, *12* (2), 518.
(29) Kawase, T.; Sawada, H. *J. Adhes. Sci. Technol.* **2002**, *16* (8), 1103.
(30) Fowkes, F. M. *J. Phys. Chem.* **1962**, *66*, 382.
(31) Girifalco, L. A.; Good, R. J. *J. Phys. Chem.* **1957**, *61*, 904.
(32) Fowkes, F. M. *Ind. Eng. Chem.* **1964**, *56*, 40.
(33) Hsieh, C. T.; Chen, J. M.; Kuo, R. R.; Lin, T. S.; Wu, C. F. *Appl. Surf. Sci.* **2005**, *240* (1−4), 318.
(34) Tsujii, K.; Yamamoto, T.; Onda, T.; Shibuichi, S. *Angew. Chem., Int. Ed.* **1997**, *36* (9), 1011.
(35) Shibuichi, S.; Yamamoto, T.; Onda, T.; Tsujii, K. *J. Colloid Interface Sci.* **1998**, *208* (1), 287.
(36) Liu, Y. Y.; Chen, X. Q.; Xin, J. H. *Nanotechnology* **2006**, *17* (13), 3259.
(37) Jung, D. H.; Park, I. J.; Choi, Y. K.; Lee, S. B.; Park, H. S.; Ruhe, J. *Langmuir* **2002**, *18* (16), 6133.
(38) Hikita, M.; Tanaka, K.; Nakamura, T.; Kajiyama, T.; Takahara, A. *Langmuir* **2006**, *21*, 7299.
(39) Zimmermann, J.; Rabe, M.; Artus, G. R. J.; Seeger, S. *Soft Matter* **2008**, *4*, 450.
(40) Nicolas, M.; Guittard, F.; Geribaldi, S. *Langmuir* **2006**, *22*, 3081.
(41) Tuteja, A.; Choi, W. J.; Ma, M.; Mabry, J. M.; Mazzella, S. A.; Rutledge, G. H.; McKinley, G. H.; Cohen, R. E. *Science* **2007**, *318*, 1618.
(42) Tuteja, A.; Choi, W. J.; McKinley, G. H.; Cohen, R. E.; Rubner, M. F. *MRS Bull.* **2008**, *33* (8), 752.
(43) Cao, L. L.; Price, T. P.; Weiss, M.; Gao, D. *Langmuir* **2008**, *24* (5), 1640.
(44) Brewer, S. A.; Willis, C. R. *Appl. Surf. Sci.* **2008**, *254* (20), 6450.
(45) Hoefnagels, H. F.; Wu, D.; de With, G.; Ming, W. *Langmuir* **2007**, *23*, 13158.
(46) Yeh, J. T.; Chen, C. L.; Huang, K. S. *J. Appl. Polym. Sci.* **2007**, *103* (5), 3019.
(47) Leng, B.; Shao, Z.; de UIT, G.; Ming, W. *Langmuir* **2009**, *25* (4), 2456.
(48) Tomsic, B.; Simoncic, B.; Orel, B.; Cerne, L.; Tavcer, P. F.; Zorko, M.; Jerman, I.; Vilcnik, A.; Kovac, J. *J. Sol−Gel Sci. Technol.* **2008**, *47* (1), 44.
(49) Liu, Y. Y.; Wang, R. H.; Lu, H. F.; Li, L.; Kong, Y. Y.; Qi, K. H.; Xin, J. H. *J. Mater. Chem.* **2007**, *17* (11), 1071.
(50) Liu, J. Q.; Shao, J. Z.; Wang, G. M.; Lu, S. F.; Fan, Q. G. *Acta Polym. Sin.* **2007**, *1*, 75.
(51) Chaudhury, M. K. *Mater. Sci. Eng.* **1996**, *R16*, 97..
(52) Vaidya, A. A.; Norton, M. L. *Langmuir* **2004**, *20* (25), 11100.
(53) Chaudhury, M. K.; Whitesides, G. M. *Langmuir* **1991**, *7*, 1013.
(54) Ferguson, G. S.; Chaudhury, M. K.; Sigal, G. B.; Whitesides, G. M. *Science* **1991**, *253*, 776.
(55) Chaudhury, M. K.; Whitesides, G. M. *Science* **1992**, *255*, 1230.
(56) Bernard, A.; Delamarche, E.; Schmid, H.; Michel, B.; Bosshard, H. R.; Biebuyck, H. *Langmuir* **1998**, *14*, 2225.
(57) Malpass, C. A.; Millsap, K. W.; Sidhu, H.; Gower, L. B. *J. Biomed. Mater. Res.* **2002**, *63* (6), 822.
(58) Manca, M.; Cortese, B.; Viola, I.; Aricò, A. S.; Cingolani, R.; Gigli, G. *Langmuir* **2008**, *24* (5), 1833.
(59) Dow Corning's products information Sylgard-184.
(60) Chi-Ming, C. *Polymer Surface Modification and Characterization*; Hanser: New York, 1994.
(61) Crist, B. V. *Handbook of Monochromatic XPS Spectra: Polymers and Polymers Damaged by X-rays*; John Wiley and Sons: Chichester, U.K., 2000.
(62) Beamson, G.; Briggs, D. *High Resolution XPS of Organic Polymers: The Scienta ESCA 300 Databses*; John Wiley and Sons: Chichester, U.K., 1992.
(63) Ferguson, G. S.; Chaudhury, M. K.; Biebuyck, H. A.; Whitesides, G. M. *Macromolecules* **1993**, *26* (22), 5870.
(64) Sui, G.; Wang, J.; Lee, C. C.; Lu, W.; Lee, S. P.; Leyton, J. V.; Wu, A. M.; Tseng, H. R. *Anal. Chem.* **2006**, *78* (15), 5543.
(65) Costa, C. A. R.; Leite, C. A. P.; Galembeck, F. *J. Phys. Chem. B* **2003**, *107* (20), 4747.
(66) Stöber, W.; Fink, A.; Bohn, E. *J. Colloid Interface Sci.* **1968**, *26*, 62.
(67) Wenzel, R. N. *Ind. Eng. Chem.* **1936**, *28*, 988.
(68) Cassie, A. B. D.; Baxter, S. *Trans. Faraday Soc.* **1944**, *40*, 546.

AM9004732